Arabian Journal of Chemistry (2009) **2**, 109–117

King Saud University

Arabian Journal of Chemistry

www.ksu.edu.sa
www.sciencedirect.com

ORIGINAL ARTICLE

Metal complexes of gliclazide: Preparation, spectroscopic and thermal characterization. Biological potential study of sulphonylurea gliclazide on the house fly, *Musca domestica* (Diptera – Muscidae)

Gehad G. Mohamed [a], Sayed M. Abdallah [b], M.M.I. Nassar [c], M.A. Zayed [a,*]

[a] *Chemistry Department, Faculty of Science, Cairo University, 12613 Giza, Egypt*
[b] *Workers University, Aswan, Egypt*
[c] *Insecticide Department, Faculty of Science, Cairo University, 12613 Giza, Egypt*

Received 13 May 2009; accepted 18 July 2009
Available online 27 October 2009

KEYWORDS

Gliclazide;
Metal complexes;
Spectroscopy;
Magnetic moment;
Thermal analyses;
Biological activity

Abstract Metal complexes of gliclazide (GLZ; HL) drug are prepared and characterized based on elemental analyses, IR, diffused reflectance, magnetic moment, molar conductance and thermal analyses (TG and DTG) technique. From the elemental analyses data, the complexes are proposed to have the general formulae $[M(HL)Cl_3(H_2O)]\cdot 3H_2O$ (M = Cr(III) and Fe(III)), $[M(HL)Cl_2(H_2O)_2]\cdot yH_2O$ (M = Co(III), Ni(II) and Cu(II), y = 0–2) and $[M(HL)Cl_2]\cdot yH_2O$ (M = Mn(II) and Zn(II), y = 0–1). The molar conductance data reveal that all the metal chelates are non-electrolytes. IR spectra show that GLZ is coordinated to the metal ions in a neutral bidentate manner with ON donor sites of the amide-*O* and sulphonamide-*OH*. From the magnetic and solid reflectance spectra, it is found that the geometrical structures of these complexes are octahedral (Cr(III), Fe(III), Co(II), Ni(II) and Cu(II)) and tetrahedral (Mn(II) and Zn(II)). The thermal behaviour of these chelates is studied using thermogravimetric analysis (TG and DTG) techniques. The results obtained show that the hydrated complexes lose water molecules of hydration followed immediately by decomposition of the anions and ligand molecules in the successive unseparate steps. The activation thermodynamic parameters are calculated using Coats–Redfern method. The GLZ drug, in comparison to its metal complexes also is screened for their biological activity against house fly, *Musca domestica*

* Corresponding author.
E-mail address: mazayed429@yahoo.com (M.A. Zayed).

1878-5352 © 2009 King Saud University. All rights reserved. Peer-review under responsibility of King Saud University.
doi:10.1016/j.arabjc.2009.10.006

Production and hosting by Elsevier

(Diptera – Muscidae). Dose of 5 μg/insect of gliclazide is typically applied against 3 days-old larval instar of *M. domestica*. Survival of pupal and adult stages has been affected by the complexes of gliclazide more than larval instars. Morphogenic abnormalities of larvae, pupae and adults are studied. On the other hand, pupation and adult emergence program is deteriorated by the effect of different chemicals.

© 2009 King Saud University. All rights reserved.

1. Introduction

Currently the most commonly prescribed medications for Type 2 diabetes were metformin and the second generation sulfonylureas which included glipizide, GLZ, glibenclamide and glimperide. For many patients with Type 2 diabetes, monotherapy with an oral antidiabetic agent was not sufficient to reach target glycaemic goals and multiple drugs may be necessary to achieve adequate control (Martha et al., 2000). In such cases, a combination of metformin and one of the sulfonylureas (SU) was used (Tack and Smits, 1999). The measurement of the plasma concentrations of antidiabetic medications was important for studying the pharmacokinetics of these drugs, for adherence and drug monitoring in diabetic patients and for diagnostic purposes in factitious hypoglycaemia. Thus, for certain diabetic populations there could be patients who were prescribed glipizide, GLZ, glimperide, glibenclamide, metformin or a combination of metformin and one of the sulfonylureas.

Several procedures had been developed to be used as standard methods for the analysis of sulfonylureas (Paroni et al., 2000; Sved et al., 1976; Sener et al., 1995; Strausbauch et al., 1995). However, none of these methods were suitable for routine analysis. Some of them used solvent extraction in sample preparation (Sved et al., 1976; Sener et al., 1995; Strausbauch et al., 1995) which is a time consuming process and loss of sample may frequently occur during extraction due to emulsion formation. In addition to that low recovery has been reported. There is no single published method for the simultaneous determination of both metformin and any of the sulfonylureas in biological fluids.

A method for determination of metformin and glipizide or GLZ (Vasudevan et al., 2001) and a method for the estimation of metformin and glibenclamide from their combined dosage forms (Khanolkar and Shinde, 1999) had been described previously for use in studying pharmaceutical preparations but not for the analysis in biological fluids. When studying the pharmacokinetics of a new formulation containing a combination of metformin and glibenclamide Martha et al. (2000) used two separate methods, one for measuring the concentration of metformin and the other for glibenclamide.

Many drugs possessed modified pharmacological and toxicological properties when administered in the form of metallic complexes. Probably the most widely studied cation in this respect was Cu(II), since a host of low-molecular-weight Cu(II) complexes had been proven beneficial against several diseases such as tuberculosis, rheumatoid, gastric ulcers, and cancers (Sorenson, 1976; Ruiz et al., 1995).

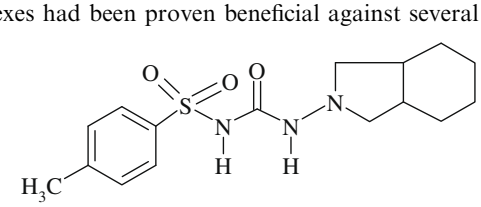

Figure 1 Structure of GLZ (HL) drug.

However, in this work we prepare chelates of Mn(II), Cr(III), Fe(III), Co(II), Ni(II), Cu(II) and Zn(II) transition metals with GLZ drug molecule. The solid chelates are characterized using different physico-chemical methods like elemental analyses (C, H, N, S and metal content), IR, magnetic moment and reflectance spectra, and thermal analyses (TG and DTG). Biological activities of the complexes are studied. The structure of GLZ drug is given in Fig. 1.

2. Experimental

2.1. Materials and reagents

All chemicals used were of the analytical reagent grade (AR), and of highest purity available. They included gliclazide (Uni-Pharma); copper(II) chloride dihydrate (Prolabo); cobalt(II) and nickel(II) chlorides hexahydrates (BDH); zinc(II) chloride dihydrate (Ubichem), chromium(III) chloride hexahydrate (Sigma); manganese(II) chloride and ferric(III) chloride hexahydrate (Prolabo). Zinc oxide, disodium salt of ethylenediaminetetraacetic acid; EDTA; (AnalaR), ammonia solution (33% v/v) and ammonium chloride (El-Nasr pharm. Chem. Co., Egypt). Organic solvents used included absolute ethyl alcohol, diethylether, and dimethylformamide (DMF). These solvents were spectroscopic pure from BDH. Hydrogen peroxide, hydrochloric and nitric acids (MERCK) were used. Deionized water collected from all glass equipments was usually used in all preparations.

2.2. Instruments

The molar conductance of solid complexes in DMF was measured using Sybron–Barnstead conductometer (Meter-PM.6, E = 3406). Elemental microanalyses of the separated solid chelates for C, H, N and S were performed at the Microanalytical Center, Cairo University, using CHNS-932 (LECO) Vario Elemental Analyzers. The analyses were repeated twice to check the accuracy of the data. Infrared spectra were recorded on a Perkin–Elmer FT-IR type 1650 spectrophotometer in wave number region 4000–400 cm^{-1}. The spectra were recorded as KBr pellets.

The solid reflectance spectra were measured on a Shimadzu 3101pc spectrophotometer. The molar magnetic susceptibility was measured on powdered samples using the Faraday method. The diamagnetic corrections were made by Pascal's constant and $Hg[Co(SCN)_4]$ was used as a calibrant. The thermogravimetric (TG and DTG) analysis was carried out in dynamic nitrogen atmosphere (20 mL min^{-1}) with a heating rate of 10 °C min^{-1} using Shimadzu TGA-50H thermal analyzer.

2.3. Synthesis of metal complexes

The metal complexes were prepared by the addition of hot solution (60 °C) of the appropriate metal chloride salts (1 mmol) in an ethanol–water mixture (1:1, 25 mL) to the hot solution (60 °C) of GLZ (0.4 g, 1 mmol) in the same solvent (25 mL). The resulting mixture was stirred under reflux for 1 h whereupon the complexes precipitated. They were collected by filtration, washed with a 1:1 ethanol:water mixture and diethyl ether. The analytical data for C, H, N and S were repeated twice.

2.4. Determination of the metal content of the chelates

An accurately weighed portion of the different chelates ranged from 10 to 30 mg was placed in Kjeldahl flask. A measured volume of concentrated nitric acid ranged from 5 to 10 mL was added initially to the powdered chelates, to start the fast wet oxidation digestion. This mixture had been digested with some drops of H_2O_2 solution using a gradual heating. This treatment was conducted until most of the powdered complexes were diminished and the remained solution had the colour of the corresponding metal salt. This solution was then diluted up to a 50 mL with bidistilled water and the metal content was determined by titration against standard EDTA solution at a suitable pH value using the suitable indicator.

2.5. Biological activity

In the present study, the larvae of *Musca domestica* were collected from the permanent colony of insect colony of Entomology Department, Faculty of Science, Cairo University. Insect were reared in the laboratory according to the method of Nassar (1988) with some modification.

2.6. Bioassay and statistical analysis

Larval mortalities were observed during the larval period, while pupal and adult mortalities were calculated based on the successfully emerged individuals from the treated larvae. The developmental rates were also studied. Data obtained were analyzed by the Student's *t*-distribution and refined by Bessel correction (Moroney, 1956).

3. Results and discussion

The formation of metal complexes with organic compounds has long been recognized. However, the binary complexes of the cited drug with metal ions have not been studied yet, although they may be an area of interest. This is because they may affect the bioavailability of these drugs as certain metal ions were present in relatively appreciable concentration in biological fluids (Salama et al., 2003).

3.1. Composition and structures of metal complexes

The isolated solid complexes of Cr(III), Mn(II), Fe(III), Co(II), Ni(II), Cu(II) and Zn(II) ions with the GLZ ligand are sub-

Table 1 Analytical and physical data of GLZ metal complexes.

Complex	Colour (% yield)	M.P. (°C)	Found (Calc. %)					μ_{eff} (B.M)	A_m (Ω^{-1} mol^{-1} cm^{-2})
			C	H	N	S	M		
$[Cr(HL)Cl_3(H_2O)]\cdot 3H_2O$ $C_{15}H_{29}Cl_3CrN_3O_7S$	Red (75)	> 300	31.91 (32.30)	5.52 (5.24)	7.20 (7.58)	6.03 (5.78)	9.09 (9.39)	4.65	13.20
$[Mn(HL)Cl_2]\cdot H_2O$ $C_{15}H_{22}Cl_2N_3MnO_4S$	Brown (70)	> 300	38.91 (38.51)	5.42 (5.78)	9.11 (8.99)	6.62 (6.85)	11.18 (11.55)	4.62	18.70
$[Fe(HL)Cl_3(H_2O)]\cdot 3H_2O$ $C_{15}H_{29}Cl_3FeN_3O_7S$	Red (78)	> 300	31.96 (32.26)	4.89 (5.20)	7.42 (7.53)	5.62 (5.74)	10.43 (10.04)	5.58	24.50
$[Co(HL)Cl_2(H_2O)_2]C_{15}H_{25}Cl_2CoN_3O_5S$	Red (68)	> 300	36.67 (36.78)	5.41 (5.11)	8.91 (8.58)	6.12 (6.54)	11.79 (12.06)	546	18.68
$[Ni(HL)Cl_2(H_2O_2]\cdot 2H_2O$ $C_{15}H_{29}Cl_2NiN_3O_7S$	Brown (77)	> 300	34.46 (34.46)	5.18 (5.18)	7.52 (7.52)	6.31 (6.31)	11.00 (11.23)	4.74	22.19
$[Cu(HL)Cl_2(H_2O_2)]C_{15}H_{25}Cl_2CuN_3O_5S$	Red (66)	> 300	36.14 (36.44)	5.21 (5.06)	8.32 (8.50)	6.19 (6.48)	12.46 (12.86)	1.98	30.10
$[Zn(HL)Cl_2]C_{15}H_{21}Cl_2N_3O_3SZn$	Red (69)	> 300	39.07 (39.18)	4.62 (4.57)	9.26 (9.14)	7.23 (6.97)	14.01 (14.15)	Diam.	20.59

jected to elemental analyses (C, H, N, S and metal content), IR, magnetic moment studies, molar conductance and thermal analyses (TG and DTG), to identify their tentative formulae in a trial to elucidate their molecular structures. The results of elemental analyses listed in Table 1 suggest the formulae $[M(HL)Cl_3(H_2O)]\cdot 3H_2O$ (M = Cr(III) and Fe(III)), $[M(HL)Cl_2(H_2O)_2]\cdot yH_2O$ (M = Co(III), Ni(II) and Cu(II), y = 0–2) and $[M(HL)Cl_2]\cdot yH_2O$ (M = Mn(II) and Zn(II), y = 0–1).

3.2. Molar conductivity measurements

The chelates are dissolved in DMF and the molar conductivities of 10^{-3} M of their solutions at 25 °C are measured. It is concluded from the results listed in Table 1 that the chelates are found to have molar conductance values of 13.20–30.10 Ω^{-1} mol^{-1} cm^2 indicating that all the metal chelates are non-electrolytes.

3.3. IR spectral studies

The IR data of the spectra of GLZ ligand and its complexes are listed in Table 2. The IR spectra of the complexes are compared with those of the free GLZ ligand in order to determine the coordination sites that may be involved in chelation. The tautomeric equilibrium depends on the extent of conjugation, nature and position of the substituents, polarity of the solvent etc.

This phenomenon has drawn considerable attention by several investigators and characteristic spectral bands have been assigned to the individual tautomers. As an example, Fig. 2 shows the IR spectrum of Zn(II) complex.

The sharp band at 1640 cm^{-1} can be assigned to the amide carbonyl of the saturated side chain moiety. A broad band spreading over the region 3400–3100 cm^{-1} can be ascribed to NH groups. Some authors have reported that the amide carbonyl group present in the saturated side chain moiety enolises. However, the strong α-effect due to heterocyclic nitrogen atom on the saturated side chain moiety prevents the enolization of this carbonyl group. The complexes under investigation have a band near 3150–3045 cm^{-1}, which is due to the N–H stretching of the saturated side chain moiety which support the presence of the amide NH in the keto form (ii) and not in the enol form (iii) (Yao and Resnick, 1962). This band is masked with a very broad band in the region 3500–3000 cm^{-1} in the spectra of the complexes under investigation which may be due to the intermolecular hydrogen bonding in the solid state.

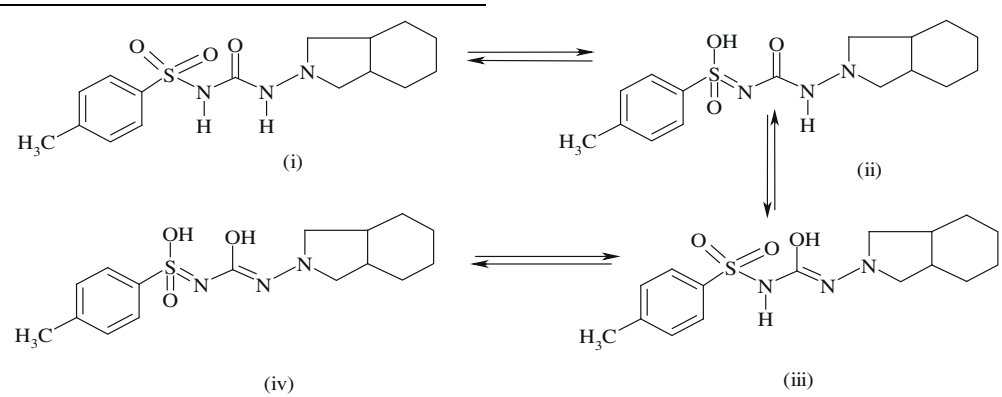

The stretching vibration band; ν(NH), of the sulfonamide group in the free ligand is hidden under the peak of water molecules or due to the enolization. The presence of coordinated water molecules renders it difficult to confirm the enolization of the sulfonamide group. The SO_2 group modes of the GLZ drug appear as sharp bands at 1375 and 1100 cm^{-1} due to $\nu_{asym}(SO_2)$ and $\nu_{sym}(SO_2)$, respectively. In the complexes, the asymmetric and symmetric modes are shifted to 1399–1410 and 1125–1160 cm^{-1}, respectively, upon coordination to the metal ions (Mohamed and Abd El-Wahwb, 2003; Raman et al., 2001). The shift of the SO_2 stretching vibration to higher frequencies may be attributed to the transformation of the sulfonamide (SO_2NH) to give the enol form (SO(OH)N) as a result of complex formation to give more stable six-membered ring (Mohamed and Abd El-Wahwb, 2003; Raman et al., 2001; Kolwalkar and Mehta, 1996). The IR bands at 815–855 and 752–770 cm^{-1}, $t(H_2O)$ of coordinated water, is an indication of the binding of the water

Table 2 IR spectra (4000–400 cm^{-1}) of the GLZ ligand and its metal complexes.

Compound	ν(OH) Enolic	ν(NH)	$\nu(SO_2)$ Asym.	$\nu(SO_2)$ Sym.	ν(C=O) Amide	ν(M–O)	ν(M–O)
GLZ;HL	3100–3400br	–	1375sh	1100sh	1460sh	–	–
$[Cr(HL)Cl_3(H_2O)]\cdot 3H_2O$	3150–3400br	3047br	1404sh	1159sh	1652m	542m	500s
$[Mn(HL)Cl_2]\cdot H_2O$	3200–3370br	3150br	1405sh	1160sh	1155sh	540m	429s
$[Fe(HL)Cl_3(H_2O)]\cdot 3H_2O$	3150–3400br	3045br	1399m	1152m	1655sh	552m	470s
$[Co(HL)Cl_2(H_2O)_2]$	3150–3400br	3045br	1410m	1160sh	1652m	550m	481s
$[Ni(HL)Cl_2(H_2O)_2]\cdot 2H_2O$	3170–3370br	3052br	1408sh	1158sh	1653m	537m	429s
$[Cu(HL)Cl_2(H_2O)_2]$	3200–3300br	3105br	1403m	1144sh	1638m	551m	425s
$[Zn(HL)Cl_2]$	3170–3450br	3059	1403m	1125m	1619sh	545s	460s

sh = sharp, m = medium, s = small, w = weak, br = broad.

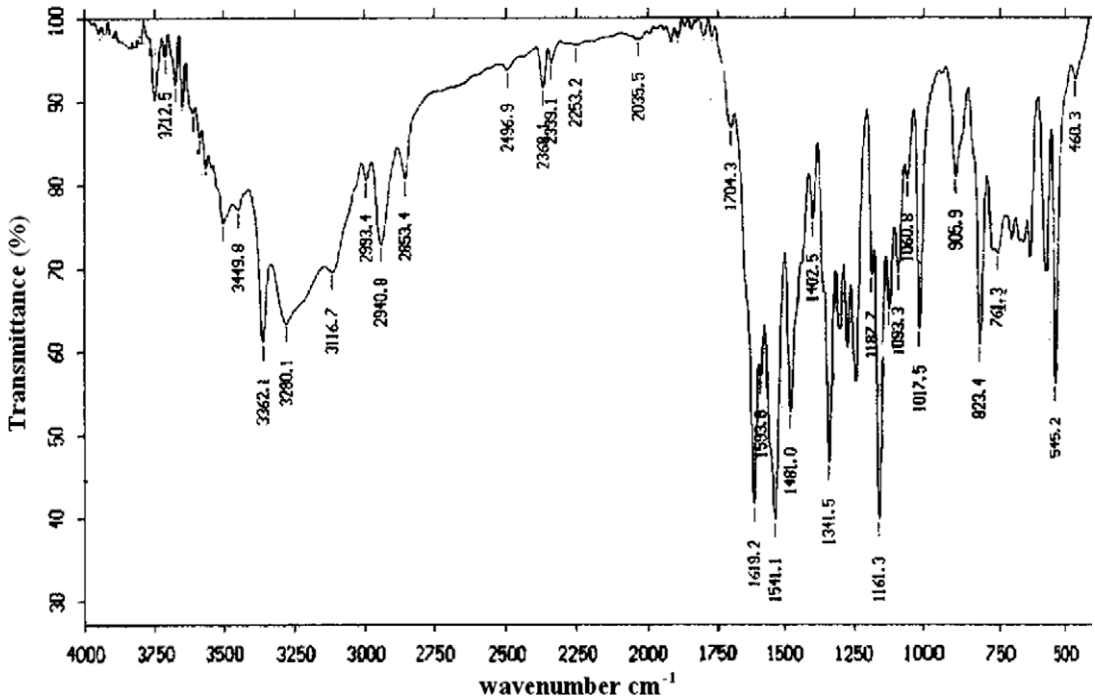

Figure 2 The FT-IR of Zn–gliclazide complex.

molecules to the metal ions. New bands are found in the spectra of the complexes in the regions 552–537 and 425–500 cm^{-1}, which are assigned to *t*(M–O) stretching vibrations of the amide and sulfonamide-O atoms (Raman et al., 2001).

Therefore, GLZ drug behaves as a neutral bidentate ligand coordinating to the metal ions via amide-*O* and enolic sulphonamide-*OH*.

3.4. Electronic spectral studies

Three spin allowed transitions at v_1: $^4A_{2g} \rightarrow {}^4T_{2g}$, v_2: $^4A_{2g} \rightarrow {}^4T_{2g}(F)$, and v_3: $^4A_{2g} \rightarrow {}^4T_{1g}(P)$ (Cotton et al., 1999) are observed for octahedral Cr(III) complex. The diffused reflectance spectrum of the Cr(III) chelate shows three absorption bands at 18,770 (v_1), 27,450 (v_2), and 28,360 cm^{-1} (v_3) which are in reasonable agreement with those in the literature for octahedral Cr(III) complexes (Cotton et al., 1999).

From the diffused reflectance spectrum it is observed that, the Fe(III) chelate exhibits a band at 22,090 cm^{-1}, which may be assigned to the $^6A_{1g} \rightarrow T_{2g}(G)$ transition in octahedral geometry of the complexes (Rosenberg et al., 1999). The $^6A_{1g} \rightarrow {}^5T_{1g}$ transition appears to be split into two bands at 16,960 and 15,450 cm^{-1} (Cotton et al., 1999). The spectrum shows also a band at 27,780 cm^{-1} which may be attributed to ligand to metal charge transfer. The diffused reflectance spectrum of the Mn(II) complex shows three bands at 15,675, 21,900 and 26,915 cm^{-1} assignable to $^6A_{1g} \rightarrow {}^4T_{1g}$, $^6A_{1g} \rightarrow {}^4T_{2g}(G)$ and $^6A_{1g} \rightarrow {}^4T_{2g}(D)$ transitions, respectively (Cotton et al., 1999), which indicates the presence of Mn(II) complex in tetrahedral structure.

The electronic spectrum of the Co(II) complex with the formula $[Co(HL)Cl_2(H_2O)_2]$ gives three bands at 14,990, 17,420 and 22,250 cm^{-1}. The bands observed are assigned to the transitions $^4T_{1g}(F) \rightarrow {}^4T_{2g}(F)$ (v_1), $^4T_{1g}(F) \rightarrow {}^4A_{2g}(F)$ (v_2) and $^4T_{1g}(F) \rightarrow {}^4T_{2g}(P)$ (v_3), respectively, suggesting the presence of Co(II) complex in octahedral geometry (Zayed et al., 2007; Cotton et al., 1999). The region at 25,660 cm^{-1} refers to the charge transfer band.

For Ni(II) complex; $[Ni(HL)Cl_2(H_2O)_2]\cdot 2H_2O$, the electronic spectrum displays three bands at v_1: 15,790 cm^{-1}: $^3A_{2g} \rightarrow {}^3T_{2g}$; v_2: 18,750 cm^{-1}: $^3A_{2g} \rightarrow {}^3T_{1g}(F)$ and v_3: 22,245 cm^{-1}: $^3A_{2g} \rightarrow {}^3T_{1g}(P)$. The spectrum shows also a band at 25,047 cm^{-1} which may be attributed to ligand to metal charge transfer (Zayed et al., 2007; Cotton et al., 1999). The reflectance spectrum of the Cu(II) chelate shows low intensity shoulder bands centered at 15,790 and 21,870 cm^{-1}. Under the influence of the tetragonal distortion, the ^2E_g and $^2T_{2g}$ states of the octahedral Cu(II) ion (d^9) split such as to cause the three transitions $^2B_{1g} \rightarrow {}^2B_{2g}$; $^2B_{1g} \rightarrow {}^2E_g$ and $^2B_{1g} \rightarrow {}^2A_{1g}$ remain unresolved in the spectra (Manonmani et al., 2000). An intense peak observed at 25490 cm^{-1} is due to ligand to metal charge transfer transition. The Zn(II) complex is diamagnetic and tetrahedral geometry is proposed for this complex.

3.5. Magnetic susceptibility studies

The room temperature magnetic moment is found to be 4.65 B.M., which corresponds to the presence of Cr(III) in octahedral geometry (Cotton et al., 1999). The observed magnetic moment value of Fe(III) complex is found to be 5.58 B.M., indicating octahedral geometry around the Fe(III) complex (Zayed et al., 2007; Cotton et al., 1999).

In addition to that, the Mn(II) complex is found to have a magnetic moment value of 4.62 B.M., which indicates the presence of Mn(II) complex in tetrahedral structure. The Co(II) complex is found to have magnetic susceptibility value of

5.46 B.M. (Table 1) which is an indicative of octahedral geometry. Meanwhile, the Ni(II) complex has a room temperature magnetic moment value of 3.74 B.M., which is in the normal range observed for octahedral Ni(II) complexes (Zayed et al., 2007; Cotton et al., 1999). The magnetic moment value of the Cu(II) complex is found to be 1.98 B.M., falls within the range normally observed for octahedral Cu(II) complexes (Manonmani et al., 2000).

3.6. Thermal analyses (TG and DTG)

In the present investigation, the weight losses for each chelate are calculated within the corresponding temperature ranges. The obtained data are listed in Table 3. $[Cr(HL)Cl_3(H_2O)]\cdot 3H_2O$ complex is thermally decomposed in three decomposition steps within the temperature range of 50–700 °C. The first

Table 3 Thermal analyses (TG and DTG) data of GLZ drug and its metal complexes.

Compound	TG range (°C)	DTG_{max} (°C)	n[a]	%Found (Calc.)		Assignment	Metallic residue
				Mass loss	Total mass loss		
$[Cr(HL)Cl_3(H_2O)]\cdot 3H_2O$	50–120	88	1	9.38(9.75)		Loss of $3H_2O$	1/2 Cr_2O_3
	120–280	202	1	40.00(39.09)		Loss of H_2O, HCl, Cl_2 and C_7H_7	
	280–700	440	1	37.85(37037)	87.23(86.21)	Loss of $C_8H_{13}N_3O_{1.5}S$	
$[Mn(HL)Cl_2]\cdot H_2O$	30–100	88	1	3.22(3.85)		Loss of H_2O	
	100–1000	14,249,656	3	81.23(80.94)	84.45(84.79)	Loss of Cl_2 and HL	MnO
$[Fe(HL)Cl_3(H_2O)]\cdot 3H_2O$	30–250	67,225	2	32.34(32.17)		Loss of Cl_2, HC1 and $4H_2O$	
	250–1000	350,620,867	3	53.22(53.67)	85.56(85.84)	Loss of HL	1/2 Fe_2O_3
$[Co(HL)Cl_2(H_2O)_2]$	100–300	215	1	41.58(41.48)		Loss of Cl_2, C_7H_{12} and $2H_2O$	
	300–800	667	1	44.09(43.11)	85.67(84.59)	Loss of $C_8H_9N_3O_2S$	CoO
$[Ni(HL)Cl_2(H_2O)_2]\cdot 2H_2O$	30–120	81	1	6.95(6.85)		Loss of $2H_2O$	
	120–250	198	1	20.18(20.75)		Loss of $2H_2O$ and 2HCl	NiO
	250–600	266,518	2	58.75(58.51)	85.88(86.11)	Loss of HL	
$[Cu(HL)Cl_2(H_2O)_2]$	100–900	235,650	2	84.49(83.90)	84.49(83.90)	Loss of Cl_2, $2H_2O$ and HL	CuO
$[Zn(HL)Cl_2]$	150–300	163	1	15.43(15.45)		Loss of Cl_2	
	300–700	430	1	66.82(66.91)	82.25(82.36)	Loss of HL	ZnO

[a] n = Number of decomposition steps.

Table 4 Thermodynamic data of the thermal decomposition of GLZ metal complexes.

Complex	Decomp. temp. (°C)	E* (k $Jmol^{-1}$)	A (s^{-1})	ΔS* (k $Jmol^{-1}$)	ΔH* (k $Jmol^{-1}$)	ΔG* (k $Jmol^{-1}$)
$[Cr(HL)Cl_3(H_2O)]\cdot 3H_2O$	50–120	32.90	1.37×10^{6}	−29.85	42.18	54.67
	120–280	53.24	2.49×10^{11}	−65.66	89.86	73.99
	280–700	109.1	4.79×10^{13}	−112.6	138.3	162.4
$[Mn(HL)Cl_2]\cdot H_2O$	30–100	33.25	1.77×10^{5}	−34.95	25.15	37.92
	100–300	82.64	3.05×10^{10}	−82.06	67.46	96.02
	300–580	142.7	4.18×10^{7}	−116.7	125.1	149.5
	580–1000	165.3	3.36×10^{11}	−136.4	160.4	162.7
$[Fe(HL)Cl_3(H_2O)]\cdot 3H_2O$	30–120	29.76	2.63×10^{6}	−24.49	48.22	58.76
	120–250	67.86	4.68×10^{11}	−66.75	85.42	117.4
	200–420	114.2	5.05×10^{9}	−116.5	148.7	165.4
	420–650	175.4	6.73×10^{13}	−147.3	177.6	199.3
	650–1000	205.6	4.89×10^{10}	−187.2	225.4	242.3
$[Co(HL)Cl_2(H_2O)_2]$	100–300	52.65	2.69×10^{9}	−43.45	45.62	69.79
	300–800	105.2	3.49×10^{11}	−98.29	116.4	141.2
$[Ni(HL)Cl_2(H_2O)_2]\cdot 2H_2O$	25–110	33.45	1.93×10^{11}	−33.96	50.48	70.46
	110–300	85.94	3.77×10^{6}	−69.17	90.79	131.3
	300–560	137.4	7.12×10^{12}	−102.2	149.2	172.6
	560–900	195.5	6.08×10^{9}	−168.4	205.3	243.7
$[Cu(HL)Cl_2(H_2O)_2]$	100–250	31.78	1.65×10^{8}	−30.94	45.66	62.66
	250–900	82.55	4.09×10^{12}	−96.47	109.3	139.0
$[Zn(HL)Cl_2]$	150–300	40.88	3.95×10^{8}	−66.74	72.66	80.96
	300–700	102.3	4.79×10^{13}	−125.4	145.3	168.7

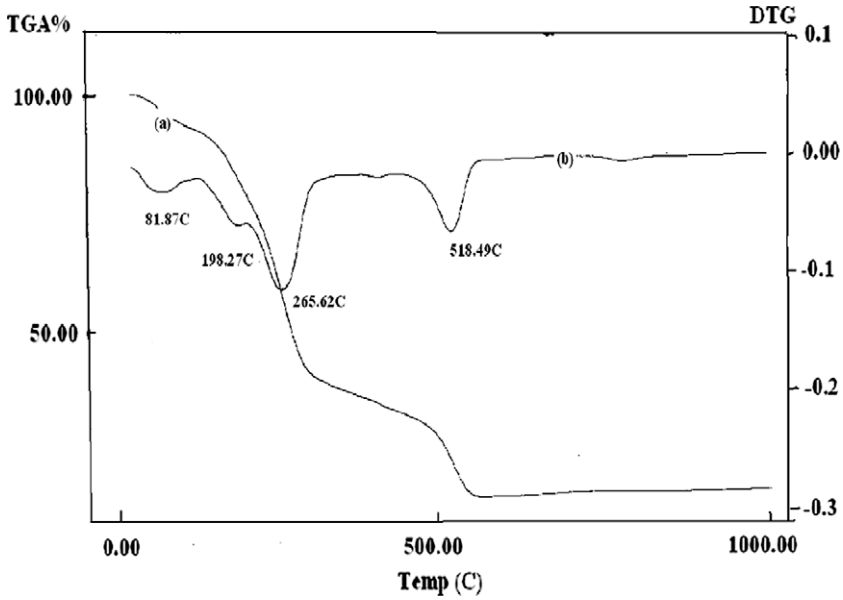

Figure 3 (a) TG of Ni–gliclazide complex, and (b) DTG of Ni–gliclazide complex.

decomposition step with an estimated mass loss of 9.38% (calc. 9.75%) within the temperature range 50–120 °C may be attributed to the liberation of three water molecules of hydration. The activation energy of this dehydration step is found to be 32.90 kJ mol^{-1}. The remaining decomposition steps were found within the temperature range 120–700 °C with an estimated mass loss of 77.85% (calc. 76.46%) can be reasonably accounted for the removal of coordinated water, HCl, Cl_2 and GLZ molecules as gases. The activation energies were listed in Table 4.

The thermogram of $[Fe(HL)Cl_3(H_2O)_2]\cdot 3H_2O$ chelate shows that the first step of decomposition within the temperature range 30–250 °C corresponds to the loss of hydrated and coordinated water molecules, Cl_2 and HCl gases with a mass loss of 32.34% (calc. 32.17%). The subsequent steps (250–1000 °C) correspond to the removal of the GLZ ligand leaving metal oxide as a residue. The overall weight loss amounts to 85.56% (calc. 85.84%).

Fig. 3 shows the TGA curve of the Ni(II) complex. The TG curves of the Mn(II) and Ni(II)-chelates show four stages of decomposition within the temperature range of 30–1000 and 30–600 °C, respectively. The stages at 30–250 °C correspond to the loss of water molecules of hydration and coordination and anions. The energy of activation for these steps is calculated using Coats–Redfern method and the data are listed in Table 4. The subsequent stages involve the loss of ligand molecules with an overall weight loss amounts to 84.45% (calc. 84.79%) and 85.88% (calc. 86.11%) for Mn(II) and Ni(II) complexes, respectively.

The TG curves of the Co(II), Cu(II) and Zn(II) chelates represent two decomposition steps as shown in Table 3. The two decomposition steps occur within the temperature range from 100–800, 100–900 and 150–700 °C and can be attributed to the loss of coordinated water, Cl_2 and GLZ molecules with an estimated mass losses of 85.76% (84.59%), 84.49% (calc. 83.90%) and 82.25% (calc. 82.36%) for Co(II), Cu(II) and Zn(II) complexes, respectively. The energy of activation for these decomposition steps are listed in Table 4. CoO, CuO and ZnO are the residues of decomposition.

3.7. Kinetic data

The thermodynamic activation parameters of decomposition processes of dehydrated complexes namely activation energy (E*), enthalpy (ΔH*), entropy (ΔS*) and Gibbs free energy change of the decomposition (ΔG*) are evaluated graphically by employing the Coats–Redfern relation (Coats and Redfern, 1964). The data are summarized in Table 4.

The activation energies of decomposition are found to be in the range 29.76–205.6 kJ mol^{-1}. The high values of the activation energies reflect the thermal stability of the complexes. The entropy of activation is found to have negative values in all the complexes which indicate that the decomposition reactions proceed with a lower rate than the normal ones.

3.8. Structural interpretation

The structures of the complexes of GLZ drug with Cr(III), Mn(II), Fe(III), Co(II), Ni(II), Cu(II) and Zn(II) ions are confirmed by the elemental analyses, IR, molar conductance, magnetic, solid reflectance and thermal analyses (TG and DTG) data. Therefore, from the IR spectra, it is concluded that GLZ drug behaves as a neutral bidentate ligand coordinated to the metal ions via the amide-*O* and sulphonamide-*OH*. The molar conductance data, it is found that the complexes are non-electrolytes. On the basis of the above observations and from the magnetic and solid reflectance measurements, octahedral and tetrahedral geometries are suggested for the investigated complexes. As a general conclusion, the complexes structures can be given as shown in Fig. 4.

3.9. Biological activity

The data show that GLZ drug under investigation and its metal complexes have the capacity of inhibiting the metabolic growth of the larvae to a different extent. The size of the inhibition zone depends upon the culture medium, incubation

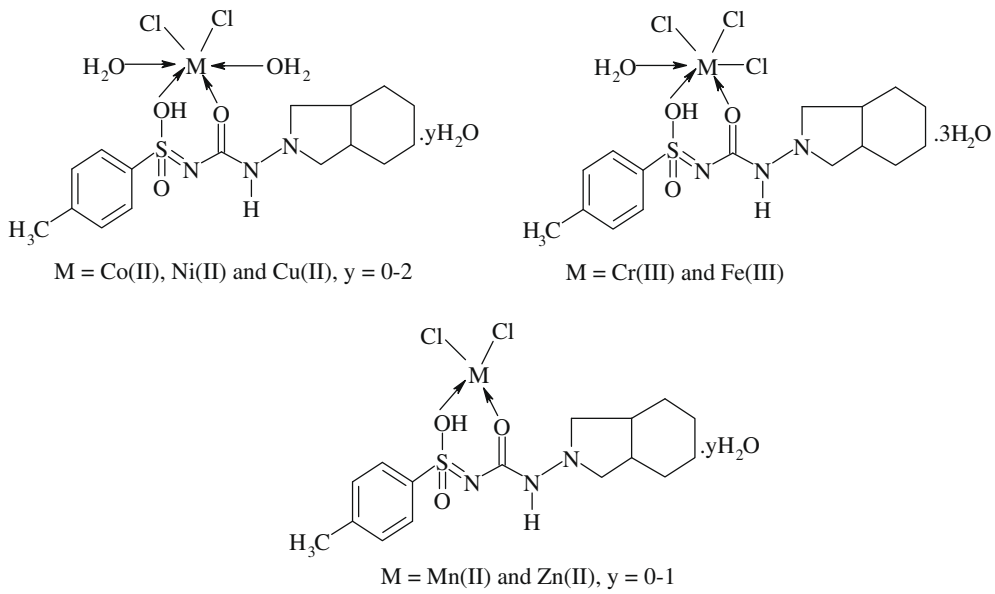

Figure 4 Structures of GLZ metal complexes.

Table 5 Effect of GLZ and its complexes on the larvae, pupae and adults mortalities of the *Musca domestica*.

Chemical compounds	Larval mortality	Pupal mortality	Adult mortality
GLZ	–	40	60
$[Mn(HL)Cl_2]\cdot H_2O$	30	40	30
$[Fe(HL)Cl_3(H_2O)]\cdot 3H_2O$	20	40	40
$[Ni(HL)Cl_2(H_2O)_2]\cdot 2H_2O$	10	80	10
Control	–	–	–

conditions, rate of diffusion and the concentration of the antibacterial agent.

The activities of all tested complexes may be explained on the basis of chelation theory: chelation reduces the polarity of the metal atom mainly because of the partial sharing of its positive charge with the donor groups and possible π electron delocalization within the whole chelate ring. Also, chelation increases the lipophilic nature of the central atom which subsequently favors its permeation through the lipid layer of the cell membrane (Caudhary and Singh, 2003).

In testing the biological activity of GLZ and its metal complexes, we used larvae of *M. domestica* to increase the chance of detecting antibiotic principles in the tested materials.

3.10. Lethal effects

In focusing the data recorded in Table 5, the potential effects of the different compounds of GLZ and its complexes (Mn(II), Fe(III) and Ni(II)) against the treated larvae of *M. domestica* are clear. Larval mortality is found to be 30%, 20% and 10% due to the effect of Mn(II), Fe(III) and Ni(II) complexes, respectively, whereas GLZ has no effect. While the three compounds; GLZ, Mn(II) and Fe(III), are found to cause 40% and Ni(II) complex is found to cause 80% of the pupal mortality. The higher adult mortality is found to be 60%, 40%, 30% and 10% by the effect of GLZ, Fe(III), Mn(II), and Ni(II) complexes, respectively, in comparison to 0.0% mortality of control insect (Table 5).

3.11. Morphogenic effects

Typical application of GLZ and its complexes on the different developmental stages of *M. domestica* resulted in different morphogenic abnormalities of pupation and adult emergence. On the other hand, the pupation program is impaired in different degrees by the various compounds. This effect is approximately a compound-dependent. Contrary to the previous fact, the GLZ drug has no effect on the larvae. On the other hand, the larval-pupal and adult deformations are increased by the effect of Mn(II), Fe(III) and Ni(II) complexes. The majority of the observed morphogenic effects represented as shrinking of skin with black colour and larval-pupal intermediate.

The toxicity effect of GLZ, seems to be due to the penetration of the different chemical compounds, is inversely proportional to the thickness of the insect cuticle. These results are in good agreement with those previously published (Bruck, 1979; Nassar et al., 2008; Samarasekera et al., 2004). It is clear from the data obtained that the larval instar was more tolerant to the chemical compounds than the pupal and adult stages. This can be attributed to insect size (Ikeda et al., 1979). On the other hand, toxicity effects of GLZ and its complexes can be attributed also to the decrease of blood glucose level in insect (Amin et al., 2004). Sulphonylurea drugs such as GLZ were found to inhibit fluid secretion and metabolism of *Drosophila melanogaster* fly (Evan et al., 2005). The insecticidal efficacy on 3rd larval instar and adult fecundity of *M. domestica* was due to the metabolism disturbance by the effect of *Trigonella foenum* extracts (Adel Halim and Morsy, 2006). In comparison, the variable effects of GLZ on the different developmental stages of *M. domestica* is found to be strengthen resistance for some complexes.

The complexes that found to produce morphological abnormalities can be attributed to their effects on total protein content

which inhibited the cholinesterase, esterase enzymes and alkaline acid phosphatases in the blood of the different stages of *M. domestica* (Ghoneim et al., 1992). Typical application of the GLZ complexes on the larval instars of the *M. domestica*, in the present study, resulted in pronouncedly prohibition of the pupation and adult emergence. It may be considered as a result of the haemolymph ecdysteroids. In other words, GLZ complexes are classified in the category of chitin inhibitors.

The possible morphogenic action of GLZ on the larvae, pupae and adult eclosion programmes, available data in the present study unambiguously prevailed increased deformity, approximately, by the decreasing dose-level of *M. domestica* (Nassar, 1995), *M. stabulans* (Ghoneim et al., 1992; Nassar, 1995) and *Rhynchophorus ferrugineus* (Ghoneim et al., 2007; Nassar et al., 2008).

References

Adel Halim, A.S., Morsy, T.A., 2006. J. Egypt Soc. Parasitol. 36, 329.

Amin, M.R., Mostafa, M., Rafi, K., Hossain, M.S., Hasan, M.M., Sharmin, M.L., 2004. J. Biol. Sci. 4, 323.

Bruck, E., 1979. J. Entomol. Germ. 2, 320.

Caudhary, A., Singh, R.V., 2003. Phosphorous Sulfur Silicon 178, 603.

Coats, A.W., Redfern, J.P., 1964. Nature 20, 68.

Cotton, F.A., Wilkinson, G., Murillo, C.A., Bochmann, M., 1999. Advanced Inorganic Chemistry, sixth ed. Wiley, New York.

Evan, J.M., Allan, A.K., Davis, S.A., Dow, J.A.T., 2005. J. Exp. Biol., 3771.

Ghoneim, K.S., Essa, N., Abul-Ela, R.G., Al-Morsy, A.A., Nassar, M.M.I., 1992. Al-Azhar Bull. Sci. 2, 687.

Ghoneim, K.S., Abdel-Ghaffar, Bream, A.S., Tanani, M.A., Nassar, M.M.I., 2007. J. Egypt. Acad. Soc. Environ. Develop. A Entomol. 9, 11.

Ikeda, J.K., Mau, R.F.L., Mitchell, W.C., Tamashiro, M., 1979. J. Econ. Entomol. 72, 33.

Khanolkar, D., Shinde, V., 1999. Indian Drugs 36, 739.

Kolwalkar, S.D., Mehta, B.H., 1996. Asian J. Chem. 8, 406.

Manonmani, J., Thirumurugan, R., Kandaswamy, M., Kuppayee, M., Raj, S.S.S., Ponnuswamy, M.N., Shanmugam, G., Fun, H.K., 2000. Polyhedron 19, 2011.

Martha, P., Arnold, M., Meeker, J., Greene, D., 2000. J. Clin. Pharmacol. 40, 1494.

Mohamed, G.G., Abd El-Wahwb, Z.H., 2003. J. Therm. Anal. And Cal. 73, 347.

Moroney, M.J., 1956. Facts from Figures, third ed. Penguin Books Ltd., Harmonds Worth, Middlesex.

Nassar, M.M.I., 1988. Some biological and toxicologica studies on the false stable fly, *Muscina stabulans* (Fallen) (Diptera – Muscidae). MS Thesis, Entomol. Dept. Fac. of Sci., Cairo Univ.

Nassar, M.M.I., 1995. The potential of some juvenoids, precocenes and botanical extracts for the control of *Muscina stabulans* (Falken) (Diptera – Muscidae). Unpublished Ph.D. Thesis, Fac. Sci., Cairo Univ.

Nassar, M.M.I., Ghoneim, K.S., Bream, A.S., Tanani, M.A., 2008. Inhibitory and toxicity effects of two IGRs (CGA-184699) and (CGA-59205) on the red palm weevil, *Rhynchophorus ferrugineus* (Coleoptera: Curculionidae). In: Proceeding of the Fourth Conference of Applied Entomology, Cairo Univ., 2008, pp. 82–94.

Paroni, R., Comuzzi, B., Arcelloni, C., Brocco, S., 2000. Clin. Chem. 64, 1773.

Raman, N., Kulandaisamy, A., Jeyasubramanian, K., 2001. Synt. React. Inorg. Met. Org. Chem. 31 (7), 1249.

Rosenberg, B., Lippert, B., 1999. Cisplatin. Chemistry and Biochemistry of a Leading Anticancer Drug. Verlag Chemie VCH, Basel 3.

Ruiz, M., Perello, L., Ortiz, R., Castineiras, A., Maichlemossmer, C., Canton, E., 1995. J. Inorg. Biochem. 59, 801.

Salama, F., El Abasawy, N., Abdel Razeq, S.A., Ismail, M.M.F., Fouad, M.M., 2003. J. Pharm. Biomed. Anal. 33, 411.

Samarasekera, J.K., Khambay, B.P., Hemalal, K.P., 2004. J. Nat. Prod. Res. 18, 117.

Sener, A., Akkan, A., Malaisse, W., 1995. Acta Diabetol. 32, 64.

Sorenson, J.R.J., 1976. J. Med. Chem. 19, 135.

Strausbauch, M., Xu, S., Ferguson, J., Nunez, M., Landers, J., 1995. J. Chromatogr. A 717, 279.

Sved, S., McGilveray, I., Beaudoin, N., 1976. J. Pharm. Sci. 65, 1356.

Tack, C., Smits, P., 1999. The Netherland J. Med. 55, 209.

Vasudevan, M., Ravi, J., Suresh, B., 2001. J. Pharm. Biomed. Anal. 25, 77.

Yao, H.C., Resnick, P., 1962. J. Am. Chem. Soc. 84, 3514Kaberia, F., Vickery, B., Willey, G.R., Drew, M.G.B., . J. Chem. Soc.. Perkin Trans. 2, 1622.

Zayed, M.A., Nour El-Dien, F.A., Mohamed, Gehad G., El-Gamel, Nadia E.A., 2007. J. Mol. Struct. 841, 41.